J. Agr. Sci. Tech. (2023) Vol. 25(2): 443-456

Metallophosphoesterases of *Chlamydomonas reinhardtii* and Analyses of Their Transcription Levels under Phosphate Deficiency

G. Hatice Havutcu[1], and M. Aksoy[1*]

ABSTRACT

Phosphorous (P) is an important macroelement for all organisms. However, there is a finite amount of P on Earth, therefore, new enzymes and technologies are needed for better P use in agriculture. Metallophosphoesterases are a large group of evolutionarily related proteins that are important in biotechnology. We found fourteen putative *Metallophosphoesterase* (MPA) genes in the genome of *Chlamydomonas reinhardtii*. Our RT-PCR analyses showed that some of these genes were constitutively expressed, and some were upregulated under phosphate deficiency. These results and bioinformatic analyses suggest that two of the genes (MPA11 and MPA13) are transcribed in high levels and the putative polypeptides are predicted to be secreted to extracellular space, making them ideal to be used in biotechnological applications. Phylogenetic analyses show that MPA11 and MPA13 are related to known phytases from plant species, suggesting MPA11 and MPA13 might have specific phytase activity. In light of these results, we discuss the potential of *C. reinhardtii* as a phytase producing organism for agricultural and industrial use.

Keywords: Phosphate nutrition, Phytase, Phytic acid, Phosphate.

INTRODUCTION

Phosphorous (P) is one of the essential macronutrients for growth and development of all organisms. Phytic acid (myo-inositol hexakisphosphate; $InsP_6$) is the largest P source in soil (salt form of phytic acid is referred as phytate). Phytic acid is the main P, inositol and mineral storage molecule for plants (Reddy *et al.,* 1982; Vohra and Satyanarayana, 2003). Plants cannot take up phytic acid; the P form that is taken up by plant roots is inorganic phosphate (Pi; PO_4^{3-}). Phytases (myo-inositol haxakisphosphate phosphohydrolase; E.C. 3.1.3.8 and 3.1.3.26) are phosphatases that hydrolyze Pi from phytate. Phytases released to soil by plant roots and microrganisms hydrolyze Pi from phytate and make it available for plant uptake. Hydrolysis of phytate by phytases release Pi, inositol, divalent cations and proteins (Yao *et al*., 2012). However, plant phytases found in roots often have low activity, which makes them ineffective in releasing Pi from soil phytate (Hayes *et al.,* 1999; Richardson *et al*., 2001). Using microbial fertilizers might make nutrients such as phytate bio-available for plants. Identification of native phytases from various biological sources, therefore, can contribute to phytase industry.

Seeds of plants, e.g. wheat grains, have large amounts of phytic acid as phosphate storage. However, monogastric species including poultry, pigs, fish and humans cannot produce phytases, or produce it in low quantities. Therefore, phytic acid is unavailable to these species; phytases or Pi is added as a supplement to the feed of these animals (Singh *et al*., 2011; Singh and Satyanarayana, 2015; Jing *et al.,* 2021). However, adding Pi is not sustainable, because Pi is not a renewable material (Secco *et al*., 2017). Therefore, phytases are important industrial enzymes that

[1] Department of Agricultural Biotechnology, Faculty of Agriculture, Akdeniz University, Türkiye.
*Corresponding author; e-mail: maksoy@akdeniz.edu.tr

are used in animal nutrition, food processing, and environmental resource management (Hermann *et al.,* 2019).

Metallophosphoesterases are a large group of evolutionarily related proteins. There is a common sequence motif (motif A) in all these enzymes (phosphoesterase motif); DXH-(X)$_{\sim 25}$-GDXXD-(X))$_{\sim 25}$- GNH[E/D], which contains four metal binding residues. After this motif, there is a second metallo-phosphoesterase motif (motif B); GH-(X)$_{\sim 50}$-GHXH (Klabunde *et al*., 1996, Figure 1). Second histidine of the GHXH is lost in protein phosphatases (Klabunde *et al*., 1996). Purple Acid Phosphatases (PAPs; EC 3.1.3.2) catalyze the hydrolysis of inorganic phosphorus from a broad range of phosphate monoesters and anhydrides in the pH range 4–7 (Olczak *et al*., 2003). In contrast, phytases (EC 3.1.3.8 and 3.1.3.26) are a distinct class of acid phosphatases with a high affinity for inositol hexaphosphate (phytate), and may, therefore, be particularly important for the hydrolysis of organic P sources in soils (Dermol *et al*., 2011). Phytases have been classified into four groups: (1) Purple Acid Phosphatases (PAP), function at pH 4-7, (2) Cysteine acid phosphatases, also called Protein Tyrosine Phosphatases (PTP) or Dual Specificity Phosphatases (DSP), (3) Histidine Acid Phosphatases (HAP), and (4) Beta-propeller phosphatases (alkaline phosphatases) (Mullaney and Ullah, 2003; Lei *et al*., 2013).

Green alga (*Chlamydomonas reinhardtii*) is an important model organism for basic research and biotechnology (Harris, 2001; Sasso *et al*., 2018). However, putative phytase coding genes of this alga has not been studied (Grossman and Aksoy, 2015). The purpose of this study was to identify the putative phytase encoding genes of *C. reinhardtii* using various bioinformatics tools and analyze their transcript levels under Pi sufficient and Pi deficient conditions.

MATERIALS AND METHODS

Bioinformatic Analyses

Protein sequences were retrieved through "MPA (metallophosphoesterase)" or "phytase" keyword searches in Phytozome database (https://phytozome.jgi.doe.gov/pz/portal.html). To make an alignment of the signature metallophosphoesterase motifs (Klabunde *et al*., 1996), protein sequences were aligned with ClustalW program (http://clustalw.ddbj.nig.ac.jp/index.php?lang=en) and regions containing the motifs were extracted from the whole alignment. The conserved residues of the motifs were colored manually. Cellular localization predictions were done using PredAlgo

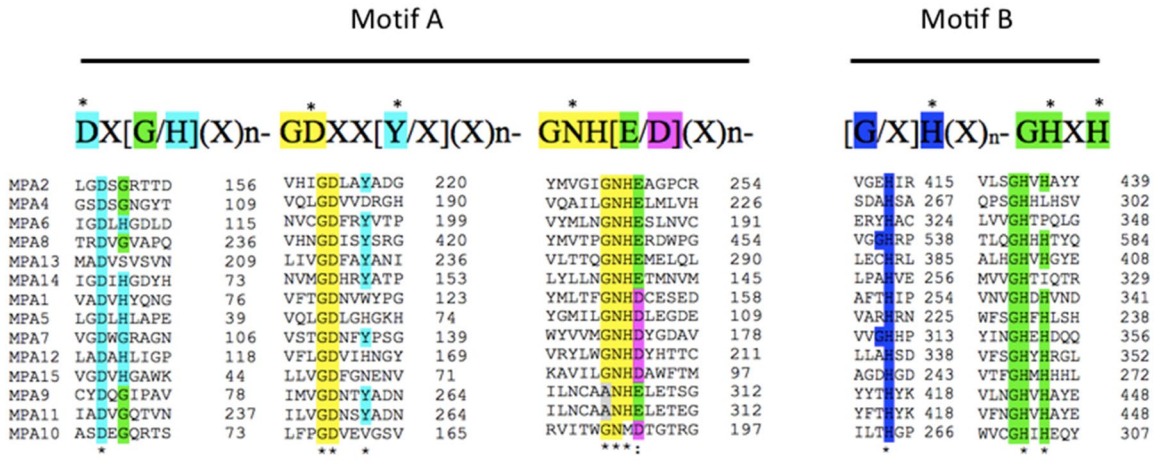

Figure 1. Conserved metallophosphoesterase motifs of MPA polypeptides. Consensus motif 1 and motif 2 of metallophosphoesterases are given on top.

Program (Tardif *et al*., 2012; http://lobosphaera.ibpc.fr/cgi-bin/predalgodb2.perl?page=main) and DeepLoc (https://services.healthtech.dtu.dk/service.php?DeepLoc-1.0). Molecular weight and isoelectric point predictions were done using Expasy database program Compute pI/Mw (https://www.expasy.org/). Signal peptide prediction was done using SignalP (Petersen *et al*., 2011; Nielsen, 2017). Transmembrane predictions were done using SMART (Simple Modular Architecture Research Tool) web resource (Letunic and Bork, 2018; http://smart.embl.de). Domain predictions were done using Pfam (Mistry *et al*., 2021) and domains were drawn using image creator MyDomians according to the instructions provided on the site (http://prosite.expasy.org/mydomains/).

Homology Modeling

Since structural similarity might suggest functional similarity, we generated homology model of all the MPAs. This could help us in predicting the functions of the MPAs and find related structural templates in the Protein Data Bank (https://www.rcsb.org/). Homology modeling was performed using the Phyre2 web portal (Kelley *et al*., 2015). Phyre2 generated all the models with 100% confidence. The models we generated were visualized with Jmol, an open-source Java viewer that represents chemical structures in three-dimensional (http://www.jmol.org/). The models generated were validated using ERRAT and Verify 3D programs (Colovos and Yeates, 1993; Eisenberg *et al.,* 1997). These were the overall quality scores from ERRAT: MPA1 (36.264), MPA2 (55.450), MPA4 (79.924), MPA5 (55.4167), MPA6 (65.591), MPA7 (52.117), MPA8 (46.035), MPA9 (35.269), MPA10 (33.594), MPA11 (41.394), MPA12 (28.148), MPA13 (56.639), MPA14 (73.106), MPA15 (52.8302). The models were also checked with Verify3D and all the models had a “pass” score, except for MPA1, 77.94% of the residues averaged 3D-1D score >= 0.2, very close to 80% treshold. Therefore, although we tested three different template models of MPA1, model generated from 2nxf template had the best scores and this was the final model used.

Phylogenetic Analyses

Amino acid sequences were aligned and the phylogenetic tree generated using ClustalW (https://www.genome.jp/tools-bin/clustalw). Alignments and phylogenetic reconstructions were performed using the function "build" of ETE3 v3.1.1 (Huerta-Cepas *et al*., 2016), as implemented on the GenomeNet (https://www.genome.jp/tools/ete/). The phylogenetic tree was constructed using fasttree with slow NNI (Nearest Neighbor Interchanges) and MLACC= 3 (to make the Maximum-Likelihood NNIs more exhaustive) (Price *et al*., 2009). Values at nodes are SH-like local support. Amino acid sequences of known PDB structures and experimentally determined phytases were also included in our analysis to determine the relatedness of *C. reinhardtii* MPAs to other taxa.

Cell Culture

Liquid cultures were grown mixotrophically in Tris Acetate Phosphate (TAP) medium (Gorman and Levine, 1965) under white fluorescent light bulbs on a shaker with 120 rpm. Light intensity was approximately 40 μmol photons m^{-2} s^{-1}. To induce phosphate or sulfate deficiency, cultures were grown as explained above until 2-4×10^6 cells mL^{-1} density. Cells were then centrifuged 5 minAUTES at 3,000×g. Media was discarded and the same volume of TA (TAP medium without phosphate) or TAP-S (TAP medium without sulfate) was added to induce phosphate or sulfate deficiencies, respectively. TA and TAP-S media were prepared according to the recipes on the Chlamydomonas Resource Center (https://www.chlamycollection.org/). Cells were completely resuspended in TA or

TAP-S medium, centrifuged again and the medium was discarded. This step was done twice to wash away phosphate or sulfate. Finally, the same volume of TA or TAP-S media was added to the cells and transferred to flasks. Flasks were again placed on a shaker as above.

RNA Isolation and RT-PCR

10-20 mL of cells were taken from above cell cultures before and after starvation at indicated time points (24 hours, 48 hours and 7 days for P starvation and 5 and 24 hours for S starvation). Cells were centrifuged at room temperature and media was removed completely using a pipet tip. Immediately, lysis buffer of NucleoSpin RNA Plant kit (Macherey-Nagel, Germany) was added to the cell pellet, mixed by 10 second vortexing and cells were placed in -80°C until RNA isolation. To isolate RNA, cells that were dissolved in the lysis buffer were disrupted by passage through a 20-gauge syringe before continuing the isolation according to the instructions provided by the manufacturer. This step was added to help rapturing the cells. RNA concentrations were measured using Biodrop (Indolab, Utama, Indonesia). Three-hundred ng total RNA was reverse transcribed using OneScript reverse transcriptase (ABM, Canada). Two µL of cDNA was the template for PCR using the GC TEMPase master mix (Ampliqon, Denmark). Primers were designed using Primer3 program (https://primer3.org/). *CBLP* gene [also Called Receptor of Activated protein Kinase C (RACK1), Phytozome accession number Cre06.g278222] was used as housekeeping gene (Chang *et al.,* 2005). Primer sequences are given in Table 1. Amplifications were performed with 95°C for 15 minutes followed by 25-40 cycles of 95°C for 30 seconds, 55°C for 40 seconds and 72°C for 40 seconds, and a final extension at 72°C for 5 minutes. PCR products were separated on a 3% agarose gel in TAE buffer. Ethidium bromide was also added to agarose gel and DNA was visualized with the UV imager MiniLumi system (DNR Bio-imaging Systems, Israel). In all reactions, a single product was generated (visualized on the agarose gel). Agarose gel image shown in Figure 3 shows a 30-cycle amplification result.

RESULTS

Bioinformatic Analyses

Through "MPA" keyword search, we found the *MPA* gene models (total fourteen) given in Table 2. "Phytase" keyword search found six hits; MPA9, MPA11 and MPA13 were again found here. However, the other three gene models (Cre08.g364100.t1.2, Cre13.g568600.t1.1, Cre09.g394350.t1.2) did not have the motifs found in metallophosphoesterases (see below), therefore, they were not analyzed any further. Although we found gene models named MPA1 to MPA15 in the Phytozome database, suggesting there are fifteen MPAs, we could not find a gene model named MPA3. Therefore, fourteen *MPA* gene models were analyzed in this work. In addition, PHOX (alkaline phosphatase), which is known to be upregulated under P deficiency (Moseley *et al*., 2009), and two other genes annotated as alkaline phosphatase (PHO1 and PHOD) were also included in our analysis (Table 2).

Using various bioinformatics tools, we obtained prediction of cellular localization, signal peptide, transmembrane domain, molecular weight and Isoelectric point (pI) of these putative MPA polypeptides (Table 2). MPA1 is likely localized in a membrane in

Table 1. List of primers used in RT-PCR analyses.

Gene	Primer	Sequence
PHOX	PHOX-E24F	*TGACTACGACGACATGACCC*
	PHOX-E25R	*GGCGCTCCACATCCACAG*
PHO1	PHO1-E7F	*TGAGTACGTTGCCATTCCCT*
	PHO1-E8R	*CAGATGGACTTGATGCGCTC*
PHOD	PHOD-E17F	*ATCTACCTGGCCATTGACGG*
	PHOD-E18R	*GATGGAGGTGTAGCGATCGA*
MPA1	MPA1-E7F	*AGCTACGACTTCATCCACCC*
	MPA1-E8R	*ATGGGGATGTGGGTGAAGG*
MPA2	MPA2-E8F	*ATCGAGGACCTGCTGCTG*
	MPA2-E9R	*CTCCTCCACGCACTTGTTG*
MPA6	MPA6-E5F	*GCATTGAGCGGCTAAACAGT*
	MPA6-E6R	*GTTCCACATCACGCTGTTGG*
MPA8	MPA8-E11F	*CGAGTGCGGTATACCCTTTG*
	MPA8-E12R	*CTCCGTGCTGTACTGTAGGA*
MPA9	MPA9-E18F	*ACCTCATGTCCGACACGTC*
	MPA9-E19R	*TTTGCTCGTGTGGTTTAGGC*
MPA10	MPA10-E2F	*AAGGGCCACGAGTGATTACA*
	MPA10-E5R	*GTGAGCCAAAGATGCGGTAC*
MPA11	MPA11-E9F	*GGTGATCTTGGTGGGAGACA*
	MPA11-E11R	*AGTTGGTGGGGAAGGAGAAG*
MPA12	MPA12-E8F	*CGTAATGGCCGTGTTCTCTG*
	MPA12-E9R	*AGTTGTCTGAGTCGTAGCGG*
MPA13	MPA13-E15F	*CTCACTCGCGACCTCAGTT*
	MPA13-3utrR	*CACGTGGGTTTATGTTCGCA*
CBLP	CBLP-F1	*CTTCTCGCCCATGACCAC*
	CBLP-R1	*CCCACCAGGTTGTTCTTCAG*

the secretory pathway (most likely plasma membrane). Cellular localization predictions obtained from PredAlgo and DeepLoc tools were similar; however, the results were different for MPA2, MPA4 and MPA7. Since SignalP also predicted a signal peptide for MPA2, most likely PredAlgo result is correct; MPA2 must be in the secretory pathway. PredAlgo prediction (secretory pathway) is more likely to be correct for MPA4 also, because although SignalP does not predict a signal peptide, smart prediction gives a transmembrane domain in N-terminus. This hydrophobic transmembrane region may indeed be a signal peptide. Also, PredAlgo result is most likely correct for MPA7; since it does not have a signal peptide, it is most likely not in the ER membrane (Table 2). Interestingly, MPA11 and MPA13 are predicted to be secreted to extracellular space. These two proteins might have a potential in biotechnological applications (see discussion).

Our motif analysis showed that all of the MPAs had the metallophosphoesterase motif (Figure 1), suggesting they are all phosphoesterases. Interestingly, some of the residues were not exactly the same, e.g. in the DXH motif; some MPAs have G instead of H and MPA13 and MPA10 do not have all of the conserved residues in motif A (Figure 1). Domain analysis showed that all of the *C. reinhardtii* MPAs had the metallophosphoesterase domain. *T. aestivum* purple acid phosphatase (PDB id 6giz) was also analyzed to check the validity of the predictions (Figure 2).

RT-PCR Analyses

RT-PCR was done using three independent cultures and similar results were obtained in all the replicates. Results of one of the replicates is shown in Figure 3-A. *CBLP* gene was used as a house keeping

Table 2. Results of bioinformatic analyses.

Phytozome accession number	Name	TM domain[a]	Localization[b]	Signal peptid	pI/MW (No of amino acids)	PDB id of the structure template/Organism the template belongs to
Cre04.g216700	PHOX	7-29	SP (Extracellular)	1-23	5.11/ 159100.92 (1491)	3zwu/*Pseudomonas fluorescens*
Cre08.g359300	PHO1	13-35	SP (Extracellular)	1-35	5.25/ 63065.89 (594)	5n1a/*Chaetomium thermophilum*
Cre05.g239850	PHOD	-	SP (Extracellular)	1-27	8.64/ 90139.97 (846)	2yeq/*Bacillus subtilis*
Cre03.g146207	MPA1	7-29	SP (ER, membrane)	1-24	6.35/ 43388.12 (402)	2nxf/*Danio rerio*
Cre12.g500200	MPA2	-	SP (M)	1-21	4.58/ 70226.11 (637)	3zk4-A/*Lupinus luteus*
Cre02.g144900	MPA 4	2-24	SP (C)	----	5.90/ 71002.80 (678)	2zbm/*Shewanella sp.*
Cre03.g152900	MPA5	-	O (M)	----	5.52/ 51083.33 (465)	2hy1/*Mycobacterium tuberulosis*
Cre03.g185200	MPA6	-	C (C)	----	6.02/ 44482.32 (414)	2zbm/*Shewanella sp.*
Cre06.g259650	MPA7	49-71	O (ER, membrane)	----	5.86/ 47919.86 (435)	3tgh/*Plasmodium falciparum*
Cre11.g468500	MPA8	7-29	SP (Extracellular)	1-28	5.66/ 75294.62 (691)	3zk4-A/*Lupinus luteus*
Cre11.g476700	MPA9	-	SP (Extracellular)	1-22	6.25/ 69228.13 (629)	6giz/*Triticum aestivum*
Cre12.g525550	MPA10	5-27	O (Mt, membrane)	----	7.92/ 37189.21 (358)	3rl4/*Rattus norvegicus*
Cre13.g578350	MPA11	-	SP (Extracellular)	1-22	6.04/ 69739.47 (632)	6giz/*Triticum aestivum*
Cre16.g657450	MPA12	-	O (Cp, membrane)	----	5.75/ 63723.64 (600)	2nxf/*Danio rerio*
Cre16.g672250	MPA13	5-24	SP (Extracellular)	1-20	8.69/ 60849.56 (557)	6giz/*Triticum aestivum*
Cre17.g718800	MPA14	-	O (Cytoplasm)	----	8.42/ 43786.73 (406)	2zbm/*Shewanella sp.*
Cre17.g729650	MPA15	-	M (M)	----	6.04/ 60588.55 (591)	3rl4/*Rattus norvegicus*

[a] Shows the predicted residues forming transmembrane domain, - indicates absence of a transmembrane domain. [b] PredAlgo predictions: DeepLoc predictions shown in parenthesis. SP: Secretory Pathway; M: Mitochondria; C: Chloroplast, O: Other.

control gene whose expression levels were shown to be constant under different growth conditions (Chang *et al*., 2005). As can be seen in Figures 3-A and -B, expression of *CBLP* is the same under all the conditions, validating our RT-PCR results. *PHOX* gene was used as the positive control, since its upregulation was shown under -P conditions (Moseley *et al*., 2009). As can be seen in Figure 3-A, *PHOX* transcription is upregulated after 24 hours Pi deficiency, and increases more after 48 hours. These results again validate our RT-PCR results. *PHO1* and *PHOD* are also annotated as alkaline phosphatases in the Phytozome database. We checked the transcription levels of these genes, since they might be involved in P metabolism. *PHO1* is highly upregulated under -P conditions, however, *PHOD* expression is very low, if any (Figure 3-A). We did not check the transcription levels of *MPA5*, *MPA7*, *MPA14* and *MPA15* gene models (see discussion).

RT-PCR results show that *MPA13*, *MPA1* and *MPA2* are only transcribed under -P conditions. Transcript of these genes could

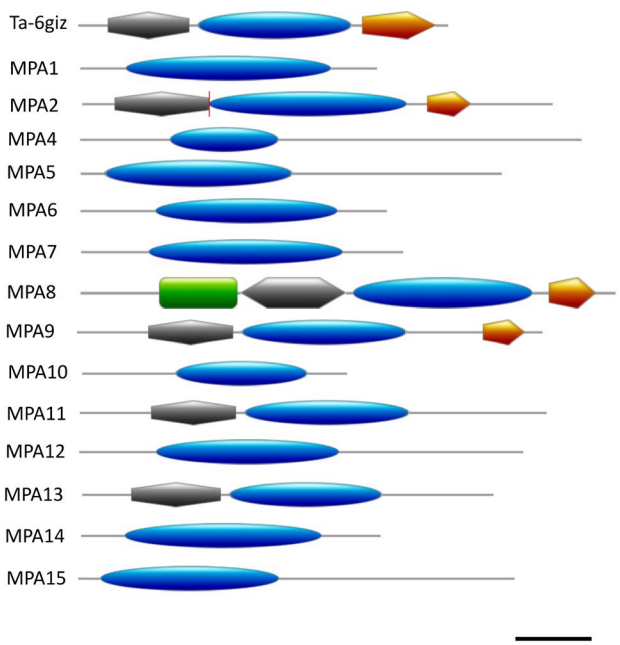

Figure 2. Domain analyses. Purple acid phosphatase N-terminal domain, black hexagon; Metallophos (calcineurin like phosphoesterase), blue elips; Metallophos C (Iron/zinc purple acid phosphatase-like protein C), orange pentagon; FN3 (Fn3-like domain from purple acid phosphatase), green rectangle. Scale bar, 100 amino acids. Ta-6giz; PDB structure for *Triticum aestivum* purple acid phytase.

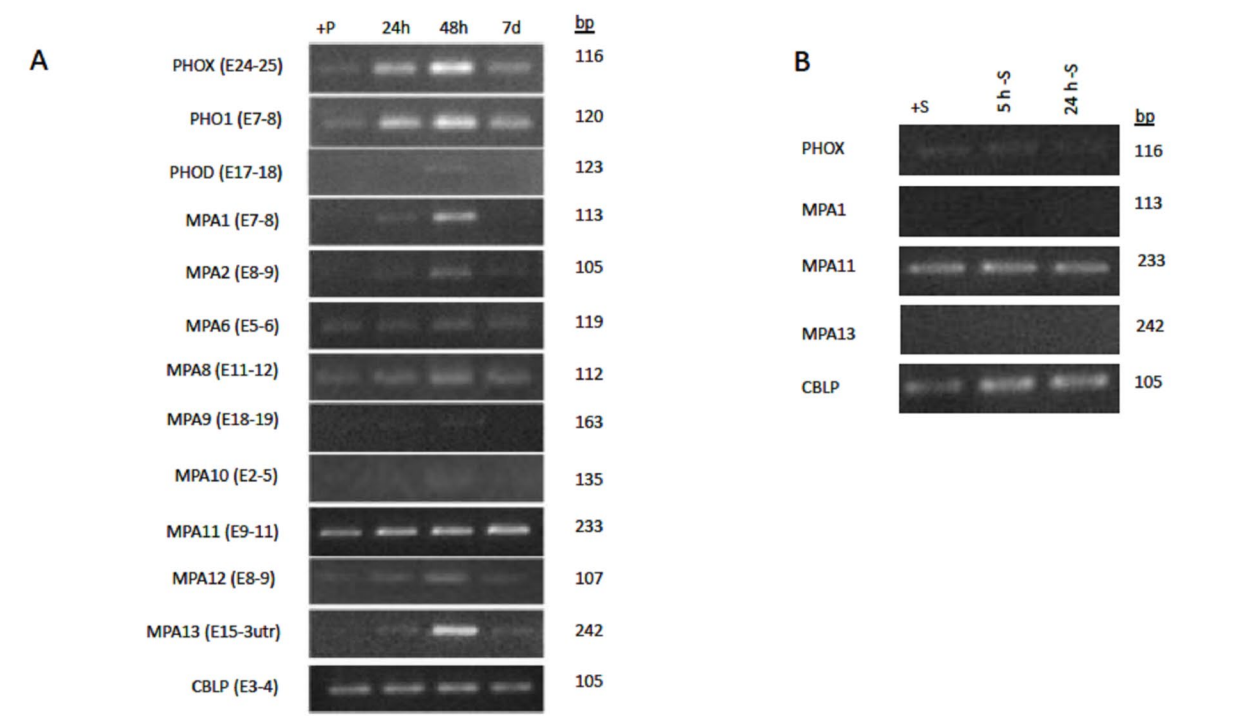

Figure 3. RT-PCR analyses: **(A)** Transcription levels under full nutrient (+P), 24 hours, 48 hours and 7 days P deficiency, and **(B)** Transcription levels under full nutrient (+S), 5 and 24 hours S deficiency. Information in parenthesis next to gene symbols shows in which exons the primers bind.

not be detected under +P in our work. The highest upregulation is seen for *MPA13*, than *MPA1* and *MPA2*, from high to low respectively (Figure 3-A). *MPA9* and *MPA10* were also upregulated, although their expression was very low (Figure 3-A). Transcription of *MPA6* looks similar under +P and -P conditions (Figure 3-A). These results suggest that MPA6 is constitutively expressed and has no involvement in acclimation to Pi deficiency. *MPA8*, *MPA11* and *MPA12* are transcribed under +P, and their expression increases slightly under -P conditions. Notably, *MPA11* is one of the genes with high expression levels (Figure 3-A). For all the upregulated genes, the increase was seen in 24 hours, continued to increase at 48 hours, and decreased at day 7. Interestingly, *MPA11* transcription stayed high even at day 7.

To determine if the MPA upregulation was specific for P deficiency, we analyzed the transcription levels under S deficiency. For this analysis, *MPA*s, which had highest upregulation under P deficiency (PHOX, MPA1, MPA11 and MPA13), were chosen. Interestingly, none of these genes had upregulation under S deficiency (Figure 3-B), suggesting their upregulation is specific for P deficiency. This result further supports the hypothesis that they might have a role in acclimation to P deficiency.

Homology Modeling

In order to gain more understanding about 3D structures of the putative MPA polypeptides, we used homology modeling. Additionally, this would allow us to find the closest structures with known functions in the PBD database. Although PHOX, PHO1 and PHOD were not our main interest, we did homology modeling of these proteins also. In fact, this proved that our approach was useful in predicting the function. These proteins are annotated as alkaline phosphatases and Phyre2 program used known alkaline phosphatases of bacterial species as structural template (Table 2).

For homology modeling of MPAs, the following templates were used:

- *Danio rerio* dimetal phosphatase (PDB id 2nxf) for MPA1 and MPA12 (Figure 4-A);
- *Lupinus luteus* purple acid phosphatase (PDB id 3zk4) for MPA2 and MPA8 (Figure 4B);
- *Shewanella sp*. (PDB id 2zbm) cold active protein tyrosine phosphatase for MPA4, MPA6 and MPA14 (Figure 4-C);
- *Mycobacterium tuberculosis* cyclic nucleotide phosphodiesterase (PDB id 2hy1) for MPA5 (Figure 4-D);
- *Triticum aestivum* purple acid phosphatase (PDB id 6giz) for MPA9, MPA11 and MPA13 (Figure 4-E);
- *Rattus norvegicus* metallophosphodiesterase (PDB id 3rl4) for MPA10 and MPA15 (Figure 4-F).

All of these templates are phosphatases, which provides evidence that *C. reinhardtii* MPAs could have phosphatase activities. Interestingly, only non-phosphatase template was *Plasmodium falciparum* cell invasion protein GAP50, a subunit of the invasion machinery or glideosome in apicomplexan parasites (PDB id 3tgh), which was used for modeling of MPA7 (Figure 4-G). However, the structure of GAP50 resembles purple acid phosphatases according to the study (Bosch *et al*., 2012).

All of the models resemble the corresponding structure template that was used by Phyre2 program and the other models generated from the same template (Figure 4). Interestingly, *C. reinhardtii* MPAs have different 3D folding suggesting they may be involved in catalysis of different substrates (Figure 4). In light of the homology modeling and phylogeny analysis results (see below), we can suggest that all the MPAs could have phosphatase activity.

Phylogenetic Analyses

Animal, plant, bacterial and apicomplexan metallophosphoesterases were included to find out *C. reinhardtii* MPAs' relatedness to other taxa and the relatedness with each other (Figure 5). The proteins from other

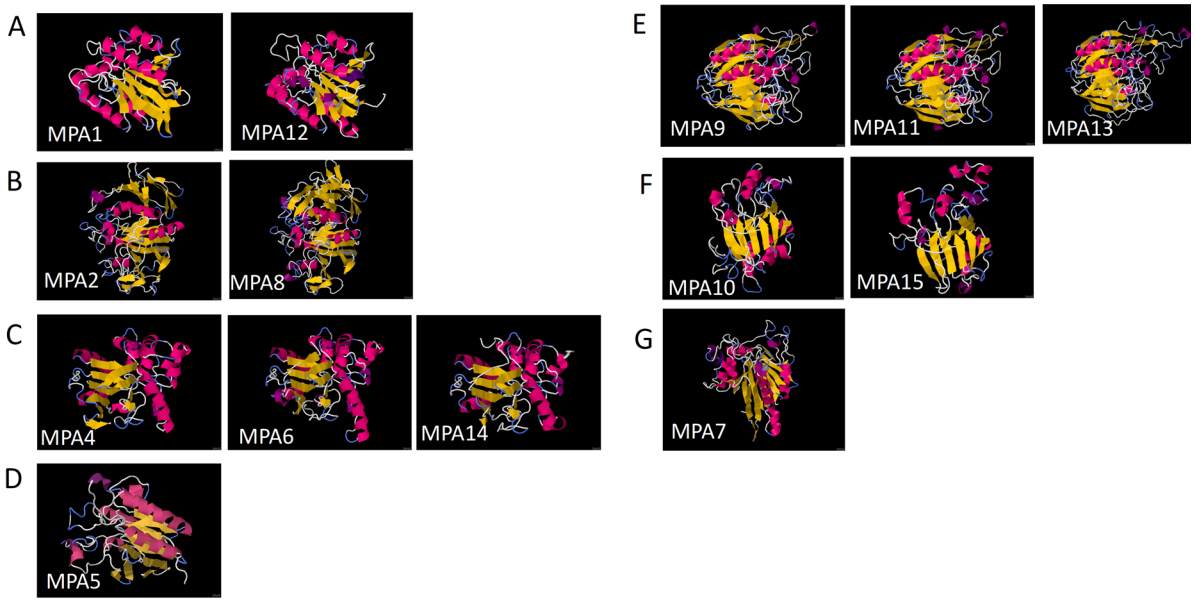

Figure 4. Predicted three-dimensional models of MPA polypeptides of *C. reinhardtii.*

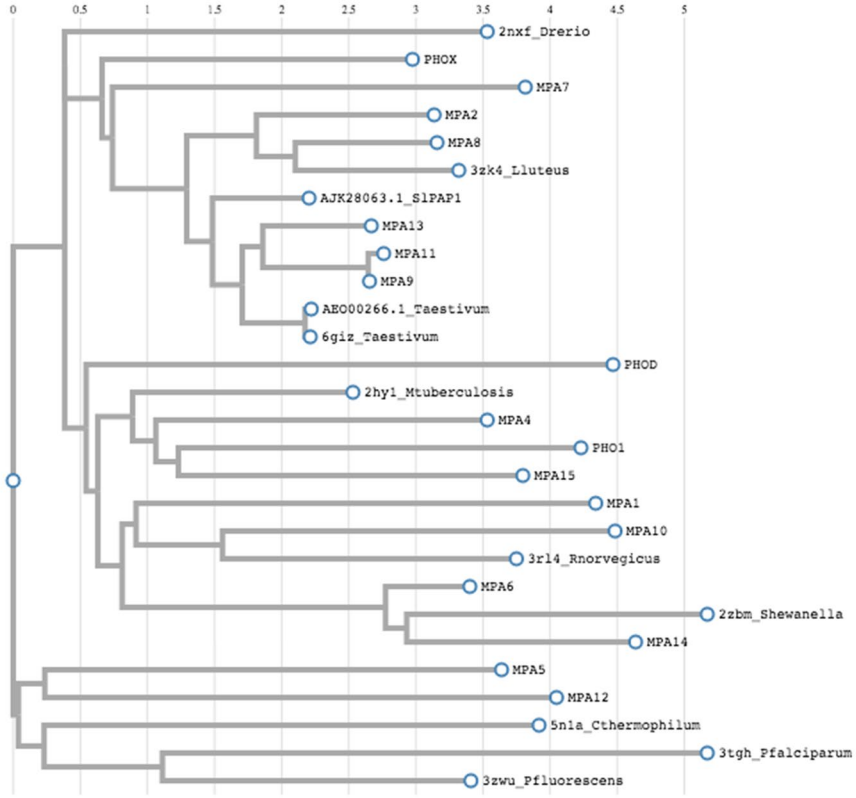

Figure 5. Phylogenetic analysis of MPA polypeptides and their relatedness to some known metallophosphoesterases.

taxa had crystal structures in PDB database and some of them also had published results that proved they had metallophosphoesterase activity (Shenoy *et al.,* 2007; Tsuruta *et al*., 2008; Dermol *et al*., 2011; Dionisio *et al*., 2011; Bosch *et al*., 2012; Antonyuk *et al*., 2014). Phylogenetic analyses show that *C. reinhardtii* has metallophosphoesterases, which are related to all the taxa that was included in our analyses. These results suggest that *C. reinhardtii* has MPAs that have different origins (Figure 5). Results show that plant metellophosphoesterases are grouped together (*T. aestivum*, 6giz; *T. aestivum*, AE000266.1; *L. luteus*, 3zk4; *S. lycopersicum*, SlPAP1) and interestingly, *C. reinhardtii* MPA13, MPA11, MPA9 are also in this group (Figure 5). MPA2 and MPA8 are grouped with another plant protein (*L.luteus,* 3zk4) and close to the other plant proteins. MPA7 is also close to the plant proteins. All the other *C. reinhardtii* MPAs are grouped together with bacterial proteins (Figure 5).

DISCUSSION

We found fourteen gene models annotated as metallophosphoesterase in the genome of *C. reinhardtii* (Table 2). We searched for the presence of signature metallophosphoesterase motif (Klabunde *et al*., 1996) in these putative polypeptides. All of them had these motifs with few amino acid substitutions, suggesting they might all have phosphoesterase activity (Figure 1).

We used RT-PCR to gain more insight about their transcription levels under Pi sufficient and Pi deficient conditions (Figure 3-A). Our results show that the highest upregulation was detected in *MPA13*, *MPA11*, *MPA1*, *MPA2* and *MPA12* (from high to low) under 48h P deficiency; the results suggest these genes are involved in acclimation to P deficiency. Our results also show that some of the MPA genes of *C. reinhardtii* are transcribed only under P deficiency and some are transcribed constitutively. Our results are in agreement with an RNA-seq study that looked at gene expression under three days Pi deficiency (Bajhaiya *et al*., 2016). This gives further support to the RT-PCR results we obtained in this study. MPA5 and MPA7 are shown to be expressed under photoautotrophic growth (Strenkert *et al*., 2019). They are not upregulated under -P conditions in an RNA-seq study (Bahjaiya *et al*., 2016). In the light of these results, most likely they are not involved in acclimation to P deficiency, therefore, we did not check the transcription levels of MPA5 and MPA7 in this study.

We used homology modeling to obtain predicted 3D models of putative MPA polypeptides to gain more insight about their functions. Homology modeling is a useful method for getting 3D structures and have been successfully used in various studies (Panahi *et al.,* 2012). These analyses showed that they had diverse structural folds (Figure 4). Eight different PDB structures (2nxf, 3zk4, 2zbm, 2hy1, 3rl4, 3tgh, 6giz, 3rl4, Table 2) were used by Phyre2 program as structural templates. All of these structural templates are known phosphoesterases (except *P. falciparum* protein, PDB id 3tgh, which might have lost the activity, however, it also has a similar structural fold as purple acid phosphatases (Bosch *et al*., 2012)).

MPA9, MPA11 and MPA13 are phylogenetically close to phytases of *T. aestivum* and *S. lycopersicum* purple acid phospahtases (Figure 5). Notably, recombinantly expressed *T. aestivum* protein (AE000266.1) was shown to have phytase activity (Dionisio *et al*., 2011). Our pairwise alignment shows that this protein is 88.1% identical to the amino acid sequence of the PDB structure 6giz (data not shown). These results suggest that *C. reinhardtii* MPA13, MPA11 and MPA9 most likely have phytase activities. Since homology modeling also used *T. aestivum* protein (Table 2, Figure. 4), this gives further support to our hypothesis that MPA9, MPA11 and MPA13 are the phytases of *C. reinhardtii*. Notably, MPA11 and MPA13 are both upregulated under P deficiency and predicted to be

secreted to extracellular space. Therefore, we suggest that they may be active in soil for phosphate hydrolysis.

Our results suggest that *C. reinhardtii* has metallophosphoesterases, which have constant expression levels (MPA6, MPA8) and some whose expression levels increase under Pi deficiency (MPA13, MPA11, MPA1, MPA2 and MPA12). Presence of these putative metallophosphoesterases would enable *C. reinhardtii* to utilize phytic acid under P sufficient and deficient conditions. This makes it a valuable microorganism in soil nutrient availability. Also, it would increase its value as a potential feed supplement in animal husbandry. MPA11 is already expressed in high levels under full nutrient conditions suggesting this enzyme might be useful in feed supplementations. MPA13 is expressed only under P deficient conditions and predicted to be secreted to extracellular space. This enzyme might be useful in soil if *C. reinhardtii* is used as a bio-fertilizer. Both MPA11 and MPA13 are predicted to be secreted, which makes it possible to be purified from liquid growth medium.

CONCLUSIONS

Our results show that *C. reinhardtii* has fourteen Metallophosphoesterase (MPA) genes. Some of these genes are constitutively expressed and some are upregulated under Pi deficiency. This gives a potential for *C. reinhardtii* to be used as a supplement in animal feed and as bio-fertilizer. MPA11 and MPA13 are highly upregulated under P deficiency (MPA11 level is already high under full nutrient conditions) and the putative polypeptides are predicted to be secreted to the extracellular space. MPA11 and MPA13 are close to known phytases, suggesting these two proteins might have phytase activity and they can be used in the phytase industry. We plan to test their specificity to phytic acid and their pH optima in our future studies.

REFERENCES

1. Antonyuk, S. V., Olczak, M., Olczak, T., Ciuraszkiewicz, J. and Strange, R. W. 2014. The Structure of a Purple Acid Phosphatase Involved in Plant Growth and Pathogen Defense exhibits a novel immunoglobulin-like fold. *IUCr J.,* **1:** 101–109.
2. Bajhaiya, A. K., Dean, A. P., Zeef, L. A. H., Webster, R. E. and Pittman, J. K. 2016. PSR1 Is a Global Transcriptional Regulator of Phosphorus Deficiency Responses and Carbon Storage Metabolism in *Chlamydomonas reinhardtii*. *Plant Physiol.,***170:** 1216–1234.
3. Bosch, J., Paige, M. H., Vaidya, A. B., Bergman, L. W. and Hol, W. G. J. 2012. Crystal Structure of GAP50, the Anchor of the Invasion Machinery in the Inner Membrane Complex of *Plasmodium falciparum*. *J. Struct. Biol*., **178:** 61–73.
4. Chang, C. W., Moseley, J. L., Wykoff, D. and Grossman, A. R. 2005. The *LPB1* Gene Is Important for Acclimation of *Chlamydomonas reinhardtii* to Phosphorus and Sulfur Deprivation. *Plant Physiol*., **138:** 319–329.
5. Colovos, C. and Yeates, T. O. 1993. Verification of Protein Structures: Patterns of Nonbonded Atomic Interactions. *Protein Sci.,* **2:**1511–1519.
6. Dermol, U., Janardan, V., Tyagi, R., Visweswariah, S. S. and Podobnik, M. 2011. Unique Utilization of a Phosphoprotein Phosphatase Fold by a Mammalian Phosphodiesterase Associated with WAGR Syndrome. *J. Mol. Biol*., **412:** 481–494.
7. Dionisio, G., Madsen, C. K., Holm, P. B., Welinder, K. G., Jørgensen, M., Stoger, E., Arcalis, E. and Brinch-Pedersen, H. 2011. Cloning and Characterization of Purple Acid Phosphatase Phytases from Wheat, Barley, Maize, and Rice. *Plant Physiol*., **156:** 1087–1100.
8. Eisenberg, D., Lüthy, R. and Bowie J. U. 1997. VERIFY3D: Assessment of Protein

Models with Three-Dimensional Profiles. *Methods Enzymol.,* **277:**396–404.
9. Gorman, D. S. and Levine, R. P. 1965. Cytochrome f and Plastocyanin: Their Sequence in the Photosynthetic Electron Transport Chain of *Chlamydomonas reinhardi*. *Proc. Natl. Acad. Sci. U. S. A*., **54:** 1665–1669.
10. Grossman, A. R. and Aksoy, M. 2015. Algae in a Phosphorus-Limited Landscape. Chapter 12. In: "*Phosphorus Metabolism in Plants*": (Edis): Plaxton, W. C. and Lambers, H. Volume 48, Annual Plant Reviews Book Series, PP. 337-374.
11. Harris, E. H. 2001. Chlamydomonas as a Model Organism. *Annu. Rev. Plant Biol*., **52:** 363–406.
12. Hayes, J. E., Richardson, A. E. and Simpson, R. J. 1999. Phytase and Acid Phosphatase Activities in Extracts from Roots of Temperate Pasture Grass and Legume Seedlings. *Aust. J. Plant Physiol*., **26:** 801–809.
13. Huerta-Cepas, J., Serra, F. and Bork, P., 2016. ETE 3: Reconstruction, Analysis, and Visualization of Phylogenomic Data. *Mol. Biol. Evol*., **33:** 1635–1638.
14. Jing, M., Zhao, S., Rogiewicz, A., Slominski, B. A. and House, J. D. 2021. Effects of Phytase Supplementation on Production Performance, Egg and Bone Quality, Plasma Biochemistry and Mineral Excretion of Layers Fed Varying Levels of Phosphorus. *Animal,* **15:** 100010.
15. Kelley, L. A., Mezulis, S., Yates, C. M., Wass, M. N. and Sternberg, M. J. E. 2015. The Phyre2 Web Portal for Protein Modeling, Prediction and Analysis. *Nat. Protoc*., **10:** 845–858.
16. Klabunde, T., Sträter, N., Fröhlich, R., Witzel, H. and Krebs, B., 1996. Mechanism of Fe(III)-Zn(II) Purple Acid Phosphatase Based on Crystal Structures. *J. Mol. Biol*., **259:** 737–748.
17. Lei, X. G., Weaver, J. D., Mullaney, E., Ullah, A. H. and Azain, M. J. 2013. Phytase: A New Life for an "Old" Enzyme. *Annu. Rev. Anim. Biosci*., **1:** 283–309.
18. Letunic, I. and Bork, P. 2018. 20 Years of the SMART Protein Domain Annotation Resource. *Nucl. Acids Res*., **46:** D493–D496.
19. Mistry, J., Chuguransky, S., Williams, L., Qureshi, M., Salazar, G. A., Sonnhammer, E. L. L., Tosatto, S. C. E., Paladin, L., Raj, S., Richardson, L. J., Finn, R. D. and Bateman, A. 2021. Pfam: The Protein Families' Database in 2021. *Nucl. Acids Res*., **49(D1):** D412–D419.
20. Moseley, J. L., Gonzalez-Ballester, D., Pootakham, W., Bailey, S. and Grossman, A. R. 2009. Genetic Interactions between Regulators Chlamydomonas Phosphorus and Sulfur Deprivation Responses. *Genetics*, **181:** 889–905.
21. Mullaney, E. J. and Ullah, A. H. J. 2003. The Term Phytase Comprises Several Different Classes of Enzymes. *Biochem. Biophys. Res. Commun.,* **312:** 179–184.
22. Nielsen, H. 2017. Predicting Secretory Proteins with SignalP. *Methods Mol. Biol*., **1611:** 59–73.
23. Olczak, M., Morawiecka, B. and Wątorek, W. 2003. Plant Purple Acid Phosphatases: Genes, Structures and Biological Function. *Acta Biochim. Pol*., **50:** 1245–1256.
24. Panahi, B., Moshtaghi, N., Torktaz, I., Panahi, A. and Roy, S. 2012. Homology Modeling and Structural Analysis of NHX Antiporter of *Leptochloa fusca* (L.). *J. Proteom. Bioinform.*, **5(9):** 214–216.
25. Petersen, T.N., Brunak, S., Von Heijne, G. and Nielsen, H. 2011. SignalP 4.0: Discriminating Signal Peptides from Transmembrane Regions. *Nat. Methods,* **8:** 785–786.
26. Price, M. N., Dehal, P. S. and Arkin, A. P. 2009. Fasttree: Computing Large Minimum Evolution Trees with Profiles Instead of a Distance Matrix. *Mol. Biol. Evol*., **26:** 1641–1650.
27. Reddy, N. R., Sathe, S. K. and Salunkhe, D. K. 1982. Phytates in Legumes and Cereals. *Adv. Food Res*., **28:** 1-92.
28. Richardson, A. E., Hadobas, P. A. and Hayes, J. E. 2001. Extracellular Secretion

of *Aspergillus* Phytase from *Arabidopsis* Roots Enables Plants to Obtain Phosphorus from Phytate. *Plant J*., **25:** 641–649.

29. Sasso, S., Stibor, H., Mittag, M. and Grossman, A. R. 2018. The Natural History of Model Organisms from Molecular Manipulation of Domesticated *Chlamydomonas reinhardtii* to Survival in Nature. *Elife*, **7:**e39233.
30. Secco, D., Bouain, N., Rouached, A., Prom-u-thai, C., Hanin, M., Pandey, A. K. and Rouached, H. 2017. Phosphate, Phytate and Phytases in Plants: From Fundamental Knowledge Gained in *Arabidopsis* to Potential Biotechnological Applications in Wheat. *Crit. Rev. Biotechnol*., **37:** 898–910.
31. Shenoy, A.R., Capuder, M., Draškovič, P., Lamba, D., Visweswariah, S. S. and Podobnik, M. 2007. Structural and Biochemical Analysis of the Rv0805 Cyclic Nucleotide Phosphodiesterase from *Mycobacterium tuberculosis. J of Mol. Biology,* **365 (1):** 211–25.
32. Singh, B., Kunze, G. and Satyanarayana, T. 2011. Developments in Biochemical Aspects and Biotechnological Applications of Microbial Phytases. *Biotechnol. Mol. Biol. Rev*., **6:** 69–87.
33. Singh, B. and Satyanarayana, T. 2015. Fungal Phytases: Characteristics and Amelioration of Nutritional Quality and Growth of Non-Ruminants. *J. Anim. Physiol. Anim. Nutr. (Berl)*., **99:** 646–660.
34. Strenkert, D., Schmollinger, S., Gallaher, S. D., Salomé, P. A., Purvine, S. O., Nicora, C. D., Mettler-Altmann, T., Soubeyrand, E., Weber, A. P. M., Lipton, M. S., Basset, G. J. and Merchant, S. S. 2019. Multiomics Resolution of Molecular Events during a Day in the Life of Chlamydomonas. *Proc. Natl. Acad. Sci. U. S. A*., **116:** 2374–2383.
35. Tardif, M., Atteia, A., Specht, M., Cogne, G., Rolland, N., Brugière, S., Hippler, M., Ferro, M., Bruley, C., Peltier, G., Vallon, O. and Cournac, L. 2012. Predalgo: A New Subcellular Localization Prediction Tool Dedicated to Green Algae. *Mol. Biol. Evol*., **29:** 3625–3639.
36. Tsuruta, H., Mikami, B., Yamamoto, C. and Yamagata, H. 2008. The Role of Group Bulkiness in the Catalytic Activity of Psychrophile Cold-active Protein Tyrosine Phosphatase. *FEBS J.* **275:** 4317–4328.
37. Vohra, A. and Satyanarayana, T. 2003. Phytases: Microbial Sources, Production, Purification, and Potential Biotechnological Applications. *Crit. Rev. Biotechnol*., **23:** 29–60.
38. Yao, M. Z., Zhang, Y. H., Lu, W. L., Hu, M. Q., Wang, W. and Liang, A. H. 2012. Phytases: Crystal Structures, Protein Engineering and Potential Biotechnological Applications. *J. Appl. Microbiol*., **112:** 1–14.

متالوفسفواسترازهای(metallophosphoesterase) موجود در *Chlamydomonas reinhardtii* و تجزیه و تحلیل سطوح رونویسی آنها تحت کمبود فسفات

گ. حدیک هاوتکو، و م. اکسوی

چکیده

فسفر (P) یک عنصر پرمصرف مهم برای همه موجودات زنده است. با این حال، مقدار محدودی از فسفر روی زمین وجود دارد، بنابراین، برای استفاده بهتر از فسفر در کشاورزی، آنزیم‌ها و فناوری‌های نوین مورد نیاز

است. متالوفسفواسترازها (metallophosphoesterase=MPA) گروه بزرگی از پروتئین های مرتبط با تکامل هستند که در بیوتکنولوژی مهم می باشند. ما چهارده ژن متالوفسفو استراز را در ژنوم *Chlamydomonas reinhardtii* یافتیم.آنالیزهای RT-PCR ما نشان داد که برخی از این ژن‌ها به گونه‌ای اساسی بیان شده-اند(constitutively expressed) و فعالیت برخی از آنها در کمبود فسفات افزایش می‌یابد (upregulated). این نتایج و تجزیه و تحلیل‌های بیوانفورماتیک چنین اشاره دارد که دو ژن (MPA11 و MPA13) در سطوح بالایی رونویسی می‌شوند و پیش‌بینی می‌شود که پلی پپتیدهای احتمالی در فضای بیرونی سلول ترشح شوند، که در نتیجه آنها برای استفاده در کاربردهای بیوتکنولوژیکی ایده‌آل می‌شوند. تجزیه و تحلیل های فیلوژنتیک نشان می دهد که MPA11 و MPA13 با فیتازهای شناخته شده از گونه های گیاهی مرتبط هستند، که نشان می دهد MPA11 و MPA13 ممکن است فعالیت فیتاز خاصی داشته باشند. با توجه به این نتایج، ما استعداد و پتانسیل *C. reinhardtii* را به عنوان یک موجود تولید کننده فیتاز برای استفاده در کشاورزی و صنعت بحث می کنیم.